

Peer Review The peer review history for this article is available as a PDF in the Supporting Information.

Key Points:

- The Psyche mission will explore the solar system's largest likely metal-rich asteroid, (16) Psyche
- Exploration of Psyche offers a historic opportunity to explore small body planetary differentiation and core formation
- The Psyche spacecraft will study Psyche using imaging, nuclear spectroscopy, magnetometry, and gravity measurements

Supporting Information:

Supporting Information may be found in the online version of this article.

Correspondence to:

S. D. Dobb and L. T. Elkins-Tanton,
dobb@baeri.org;
telkins@asu.edu

Citation:

Dobb, S. D., Asphaug, E., Bell, J. F., Binzel, R. P., Bottke, W. F., Cambioni, S., et al. (2024). A post-launch summary of the science of NASA's Psyche mission. *AGU Advances*, 5, e2023AV001077. <https://doi.org/10.1029/2023AV001077>

Received 6 OCT 2023

Accepted 26 JAN 2024

Author Contributions:

Conceptualization: Steven D. Dobb, Erik Asphaug, James F. Bell, Richard P. Binzel, William F. Bottke, Saverio Cambioni, John M. Christoph, Linda T. Elkins-Tanton, Ralf Jaumann, David J. Lawrence, Rona Oran, Joseph G. O'Rourke, Carol Polansky, Benjamin P. Weiss, Mark Wiczorek, David A. Williams

Project administration: Linda T. Elkins-Tanton, Carol Polansky, Benjamin P. Weiss

© 2024. The Authors.

This is an open access article under the terms of the [Creative Commons Attribution-NonCommercial-NoDerivs License](#), which permits use and distribution in any medium, provided the original work is properly cited, the use is non-commercial and no modifications or adaptations are made.

A Post-Launch Summary of the Science of NASA's Psyche Mission

Steven D. Dobb¹, Erik Asphaug², James F. Bell³, Richard P. Binzel⁴, William F. Bottke⁵, Saverio Cambioni⁴, John M. Christoph⁶, Linda T. Elkins-Tanton³, Ralf Jaumann⁷, David J. Lawrence⁸, Rona Oran⁴, Joseph G. O'Rourke³, Carol Polansky⁹, Benjamin P. Weiss⁴, Mark Wiczorek¹⁰, and David A. Williams³

¹Bay Area Environmental Research Institute, NASA Ames Research Center, Moffett Field, CA, USA, ²Lunar and Planetary Laboratory, University of Arizona, Tucson, AZ, USA, ³School of Earth and Space Exploration, Arizona State University, Tempe, AZ, USA, ⁴Department of Earth, Atmospheric, and Planetary Sciences, Massachusetts Institute of Technology, Cambridge, MA, USA, ⁵Department of Space Studies, Southwest Research Institute, Boulder, CO, USA, ⁶Department of Mineral Sciences, Smithsonian Institution, Washington, DC, USA, ⁷Institute of Geological Sciences, Freie Universität Berlin, Berlin, Germany, ⁸Johns Hopkins University Applied Physics Laboratory, Laurel, MD, USA, ⁹Jet Propulsion Laboratory, La Cañada Flintridge, CA, USA, ¹⁰Université Paris Cité, Institut de Physique du Globe de Paris, CNRS, Paris, France

Abstract Astronomical observations indicate that asteroid (16) Psyche is a large, high-density (likely $>3,400 \text{ kg}\cdot\text{m}^{-3}$), metal-rich (30–55 vol. %) asteroid. Psyche may be remnant core material or it could be a primordial, undifferentiated metal-rich object. We discuss the science objectives of the upcoming Psyche mission, which will employ three instruments (the Magnetometer, Multispectral Imager, and Gamma-Ray and Neutron Spectrometer) and will use Doppler tracking of the spacecraft to explore the asteroid. This mission will shed light on the nature and origins of metal-rich objects in the solar system and beyond, including the cores of the terrestrial planets.

Plain Language Summary Asteroid (16) Psyche is the largest known metal-rich asteroid and is a relic of the building blocks of the planets from the early solar system. We hypothesize that it is either an exposed metallic core of an asteroid or unmelted metal-rich material. NASA's Psyche mission, launched in October 2023, aims to explore Psyche to understand its formation and evolution. The Psyche spacecraft carries three instruments and will use its radio antenna to study Psyche's magnetic field, surface composition, and interior structure. The Psyche mission offers a historic opportunity to study the processes that led to the formation of the metallic cores of planets.

1. Psyche: An Asteroid and Mission

O Goddess! Hear these tuneless numbers, wrung
By sweet enforcement and remembrance dear
And pardon that thy secrets should be sung
Even into thine own soft-conched ear.
Surely I dreamt today, or did I see
The winged Psyche with awakened eyes?

John Keats
Ode to Psyche
Spring 1819

Asteroid (16) Psyche represents one of the last unexplored compositional classes of solar systems objects: a world likely rich in metal (Elkins-Tanton et al., 2020, 2022). Current spectral observations and density estimates of (16) Psyche (henceforth referred to as “Psyche”) suggest it to be 30–55 vol.% Fe metal, significantly higher than most chondritic meteorites, which generally have less than ~11 vol.% metal (Elkins-Tanton et al., 2020, 2022; Krot et al., 2014). Such concentrations of metal in planetary systems can form through heating and subsequent separation of metal and silicate during planetary differentiation and/or by preferential accretion of unmelted and highly reduced primordial material (Elkins-Tanton et al., 2020). Spacecraft exploration of Psyche therefore offers

Visualization: Steven D. Dobb, Linda T. Elkins-Tanton, Carol Polansky, Benjamin P. Weiss

Writing – original draft: Steven D. Dobb, Erik Asphaug, James F. Bell, Richard P. Binzel, William F. Bottke, Saverio Cambioni, John M. Christoph, Linda T. Elkins-Tanton, Ralf Jaumann, David J. Lawrence, Rona Oran, Joseph G. O'Rourke, Carol Polansky, Benjamin P. Weiss, Mark Wieczorek, David A. Williams

Writing – review & editing: Steven D. Dobb, Erik Asphaug, James F. Bell, Richard P. Binzel, William F. Bottke, Saverio Cambioni, John M. Christoph, Linda T. Elkins-Tanton, Ralf Jaumann, David J. Lawrence, Rona Oran, Joseph G. O'Rourke, Carol Polansky, Benjamin P. Weiss, Mark Wieczorek, David A. Williams

an unparalleled opportunity to study processes related to planetary differentiation and core formation. The Psyche mission, NASA's Discovery mission launched on 13 October 2023, will explore Psyche to address five science objectives:

- Determine whether Psyche is a core, or if it is primordial unmelted material.
- Determine the relative ages of regions of Psyche's surface.
- Determine whether small metal bodies incorporate the same light elements into the metal phase as are expected in the Earth's high-pressure core.
- Determine whether Psyche was formed under conditions more oxidizing or more reducing than Earth's core.
- Characterize Psyche's morphology.

The Psyche spacecraft will begin orbiting the asteroid in August 2029 to address these objectives using three instruments: the Magnetometer, Multispectral Imager, and Gamma-Ray and Neutron Spectrometer (GRNS). The mission will also measure Psyche's gravity field using Doppler tracking of the radio signals emitted by the spacecraft's communication system. Over an expected primary mission of 26 months, the spacecraft will orbit the asteroid in a series of circular orbits with varying altitudes. The orbits are lettered according to their expected altitude: Orbit A: 709 km; Orbit B: 303 km; Orbit C: 190 km; and Orbit D: 75 km. These orbital altitudes were originally designed such that the measurement requirements for the different investigations would be met at the end of each orbit (i.e., Imager objectives met in Orbit B, Magnetometer and gravity science objectives met in Orbit C, and GRNS objectives met in Orbit D). However, due to solar illumination constraints following the updated 2023 launch date for Psyche, the spacecraft will proceed through the four orbital altitudes in five phases: Orbit A, the first phase of Orbit B (named Orbit B1), Orbit D, Orbit C, and the second phase of Orbit B (named Orbit B2).

In this paper, we first discuss current observations of and hypotheses surrounding asteroid Psyche, followed by an overview of each of the Psyche mission's science objectives and how they will be met. Next, we describe the design of each of the Psyche mission's instruments. Finally, we discuss some additional possible science value expected, but not required, from the Psyche mission.

1.1. Historical and Current Observations of Psyche

Psyche was the sixteenth asteroid to be discovered and was first observed on 17 March 1852 by Italian astronomer Annibale de Gasparis at the Observatory of Capodimonte in Naples (de Gasparis, 1893; Schmadel, 2012). Analysis of the asteroid's light curve revealed a rotation period of about 4.2 hr (e.g., van Houten-Groeneveld & van Houten, 1958). Numerous measurements of the asteroid's mass and density have been reported: using published values from the past 25 years, the Psyche team has adopted a preferred mass of $(22.87 \pm 0.70) \times 10^{18}$ kg ($\sim 1\%$ of the total mass of the main asteroid belt) and density of $3,780 \pm 340$ kg·m⁻³ (Elkins-Tanton et al., 2020). This density exceeds that of many stony minerals (e.g., quartz, 2,648 kg·m⁻³; forsterite, 3,227 kg·m⁻³; enstatite, 3,270 kg·m⁻³), indicating that some higher density phase exists within Psyche (Bass, 1995). Comparison with other planetary bodies and meteorites suggests this phase is likely iron-nickel metal. Like other planetary bodies, Psyche is not spherical but rather closer to a triaxial ellipsoid. The team has adopted the dimensions from the most recent shape model from Shepard et al. (2021) with dimensions 278 (−4/+8 km) × 238 (−4/+6 km) × 171 km (−1/+5 km) and an effective spherical diameter of 222 −1/+4 km. This diameter places Psyche in the top 20 largest known asteroids (Carry, 2012).

Psyche was the first categorized and is the largest member of the “M” asteroids, which are defined by a modest visual albedo ($> \sim 0.1$ and $< \sim 0.3$) and a featureless, red-sloped visible reflectance spectrum interpreted as a surface analogous to enstatite chondrite or iron meteorites (Tholen, 1984; Zellner & Gradie, 1976). With the advent of larger scale asteroid spectral surveys at near-infrared wavelengths, subsequent observations of asteroids in the 1990s and 2000s demonstrated that previously defined taxonomic groups consist of a more continuous distribution of albedos and spectral slopes, rather than distinct clusters (e.g., Bus & Binzel, 2002; DeMeo et al., 2009). Out of this work, the “M-class” was no longer recognized as a category as spectral reflectance colors alone cannot uniquely identify “metallic” compositions. Thus, Psyche was placed into the larger X-complex of spectrally featureless asteroids which includes objects with surface reflectance similar to enstatite chondrites and iron meteorites (Bus & Binzel, 2002; DeMeo et al., 2009). Out of the 371 asteroids classified by DeMeo et al. (2009), Psyche was one of 18 Xk-type asteroids, the largest subgroup of 32 X-complex asteroids.

This new classification and other contemporaneous measurements of the asteroid were largely consistent with the original metal-rich interpretation. Near-infrared (near-IR) reflectance spectra by Hardersen et al. (2005) identified Fe-poor (<10 mol.% Fe) orthopyroxenes comprising at most 10% of Psyche's surface. Psyche's high radar albedo, a property indicative of near-surface bulk density and composition, was reported by Shepard et al. (2010) as 0.42 ± 0.10 . This is one of the highest radar albedos ever measured for an asteroid and was roughly three times the mean value for the C-type (0.13 ± 0.05) and S-type (0.14 ± 0.04) asteroids reported by Magri et al. (2007). Comparison of radar and near-IR observations of the M/X-types placed Psyche among those for which the metal-rich interpretation was most consistent (Burbine & Binzel, 2002; Bus & Binzel, 2002; Fornasier et al., 2010; Ockert-Bell et al., 2010). Although Rivkin et al. (1995) found that many M/X-type asteroids featured 3- μ m absorption consistent with hydrated minerals, Psyche notably did not, suggesting a lack of such minerals on the surface (Rivkin et al., 2000). Finally, mid-infrared (8–13 μ m) radiometry initially indicated Psyche has a high thermal inertia ($133 \pm 40 \text{ J-m}^{-2} \text{ s}^{-0.5} \text{ K}^{-1}$) and low surface roughness, consistent with a metal-rich body; however, we note that this interpretation of radiometry strongly depends on the assumed size of the body and the wavelengths used (Matter et al., 2013).

The development of the Psyche mission has prompted new Earth-based observation of the asteroid and renewed study of earlier data, which now indicate a more complex and heterogeneous surface than previously interpreted. Rotational variation of Psyche's near-IR and radar reflectance was observed, consistent with a spatially heterogeneous surface composition (Sanchez et al., 2017; Shepard et al., 2017). While the range of near-IR absorption band centers (913–960 nm) and band depths (0%–2.9%) reported for Psyche over the past ~ 20 years are consistent with a low-Fe pyroxene (e.g., enstatite) mixed with metal, Dobb et al. (2023) showed that such absorption band properties are also consistent with a more Fe-rich pyroxene (e.g., 45.6 mol.% Fe) when intimately mixed with meteoritic metal. Second, Dobb et al. (2023) showed that full visible to near-IR spectra of Psyche, while consistent with spectra of iron meteorites, are also consistent with spectra of powders from sulfides (e.g., troilite, FeS) and the metal-rich CH/CBb chondrite Isheyevo. The presence of troilite, with a density of $4,839 \text{ kg-m}^{-3}$, would be consistent with Psyche's high density and radar reflectivity (Bass, 1995). Furthermore, the best match for the asteroid's reflectance spectrum compared to that of relevant minerals varied as a function of position on the asteroid, further suggesting rotational surface heterogeneity. Ultraviolet spectra obtained using the Hubble Space Telescope by Becker et al. (2020) are consistent with metallic iron; however, they calculated that metallic iron could dominate reflectance spectra at just 10 wt.% and they identified reflectance features consistent with metal oxides. Similarly, the radar measurements reported for Psyche are consistent with a high metal content (e.g., ~ 90 wt.% metal for the solid phase, assuming $\sim 50\%$ porosity) in the uppermost meter of the surface, variably mixed with other minerals in correlation with surface topography (Ostro et al., 1985; Shepard et al., 2021). Psyche's radar albedo was shown by Shepard et al. (2021) to vary between 0.22 and 0.52 throughout the asteroid's rotation, suggesting areas of varying metal abundance. Finally, Takir et al. (2016) reported a 3- μ m absorption feature not previously identified on Psyche by Rivkin et al. (2000), which they attributed to water or hydroxyl consistent with phyllosilicates on the asteroid's surface possibly implanted by carbonaceous impactors.

Interpretations of the asteroid's surface properties from observations at longer infrared and millimeter wavelengths are still debated. Mid-IR (5–14 μ m) observations with the Spitzer Space Telescope are consistent with a fine-grained silicate regolith overlying metal-rich bedrock and a much lower thermal inertia ($5\text{--}25 \text{ J-m}^{-2} \text{ s}^{-0.5} \text{ K}^{-1}$) than previously reported, more consistent with a dusty, silicate regolith (Landsman et al., 2018). Racero et al. (2022) reported 70–500 μ m data of Psyche from the Herschel Space Observatory consistent with a thermal inertia of $20\text{--}80 \text{ J-m}^{-2} \text{ s}^{-0.5} \text{ K}^{-1}$. Finally, emissivity and polarization observations from the Atacama Large Millimeter Array (ALMA) ($\lambda = 1.3 \text{ mm}$) reported by de Kleer et al. (2021) indicate high thermal inertia ($280 \pm 100 \text{ J-m}^{-2} \text{ s}^{-0.5} \text{ K}^{-1}$) and optical scattering, consistent with a mixture of metals (including sulfides and oxides) and silicate minerals with a minimum of 20 wt.% metal for a case with no porosity, although higher metal contents are possible with higher porosity. Cambioni et al. (2022) resolved thermal anomalies in the ALMA data by varying dielectric and thermal inertia across models of Psyche's surface and concluded that a range of values for thermal inertia ($25\text{--}600 \text{ J-m}^{-2} \text{ s}^{-0.5} \text{ K}^{-1}$) and dielectric constant ($\sim 8\text{--}60$) were possible, further supporting the interpretation that Psyche's surface is a heterogeneous mixture of metal and silicates.

1.2. Hypotheses of Psyche's Formation and Evolution

Even with the wealth of data from remote observations, Psyche's formation remains unclear. Our fiducial hypothesis for Psyche's formation is that it is the core of a differentiated planetesimal that was stripped of its silicate

mantle by one or more catastrophic collisions (Elkins-Tanton et al., 2022). Within 0.5 million years of the formation of the first solar system solids, planetesimals 10–100 km in size are thought to have accreted, melted due to heating from radiogenic ^{26}Al , and differentiated into a silicate mantle and a metallic core (e.g., Weiss & Elkins-Tanton, 2013). Later, many planetesimals collided, with asteroids the size of Psyche likely near the threshold separating a surviving primordial population and a population that would be subject to disruption (O'Brien & Greenberg, 2003). As such, Psyche may have survived catastrophic disruption but lost a substantial fraction of its mantle in the process. More recent theories suggest that Psyche could be the remnant material from the metallic core of the impactor (rather than the target) in a hit-and-run style collision (Asphaug & Reufer, 2014; Gabriel & Cambioni, 2023). In this scenario, the mantle of the proto-Psyche impactor would be stripped and accreted by the target body, while the metal-rich core material may escape and survive as a runner to become what we see as Psyche today (e.g., Gabriel & Cambioni, 2023). The erosion of proto-Psyche's silicate mantle in this way could explain the observed lack of spectral features consistent with Fe-bearing olivine (a typical mantle material) on Psyche's surface and the lack of a dynamical family linked to Psyche (Binzel et al., 1995; Burbine et al., 1996; Dobb et al., 2023; Sanchez et al., 2017).

An alternative theory is that Psyche accreted from highly reduced, primordial metal-rich materials and never melted or differentiated (Elkins-Tanton et al., 2022). If this is true, Psyche likely represents the largest accessible concentrated agglomeration of primordial metal in the solar system. The question then becomes where such objects could form in the solar nebula. Iron-rich materials, including both Fe,Ni alloys and more oxidized Fe-bearing silicates (e.g., ferrosilite and fayalite), are thought to be abundant in the innermost part of protoplanetary disks (<1.0 AU; Aguichine et al., 2020). Meteoritic analogs for these materials may include H and enstatite chondrites which contain significant metal (<20 vol.%), although less than what is inferred for Psyche (Krot et al., 2014). In contrast, other iron-rich meteorites, such as CH and CB chondrites, have been linked to carbonaceous chondrites, which likely formed beyond the orbit of Jupiter (Johnson et al., 2016; Kruijer et al., 2017). Given that most of the large (diameter >40 km) M/X-type asteroids orbit the Sun in the central and outer main asteroid belt, it is possible that M/X-types originated beyond the main-belt and were then implanted there by early solar system processes (Kruijer et al., 2020). However, the CB chondrites are themselves inferred to have formed during an impact between planetary embryos (e.g., Garvie et al., 2017; Krot et al., 2005). If the mission demonstrates that Psyche is CB-like, it will further indicate that growing planetary systems experience significant orbital mixing, complicating typical interpretation of expected chemical gradients in a protoplanetary disk.

While Psyche is likely the largest metal-rich asteroid and likely has a metal-rich surface, it is not the largest metal-rich world. Our own planet's core ($\sim 1/3$ of its mass) has been studied for decades yet remains the target of research into core structure, dynamics, and composition (e.g., Hirose et al., 2021). Like Psyche, Mercury's anomalously large core (accounting for $\sim 70\%$ of its mass) has a similarly elusive origin (Ebel & Stewart, 2018). Finally, the discovery of ~ 10 – 15 high-density exoplanets suggests that metal-rich worlds may be a common product of planet formation (Adibekyan et al., 2021; Unterborn et al., 2023). Psyche's metallic surface, in contrast to exoplanets or the cores of Earth and Mercury, is accessible via spacecraft. Hence, the Psyche mission is an unparalleled opportunity to understand how planetary cores form and evolve.

2. The Five Science Objectives of the Psyche Mission

The broad goal of the Psyche mission is to explore a previously unexplored building block of planetary formation: an iron core. From this overarching goal, five scientific objectives have been designed to guide the development of the spacecraft payload.

2.1. Determine if Psyche Is a Core, or if It Is Primordial Unmelted Material

As described in Section 1, current observations of Psyche indicate it is one of the most likely metal-rich objects readily accessible in the Solar System. The main motivation for making high-resolution measurements of Psyche from an orbiter is to first determine if it is a metal-rich world and to test the hypothesis that it is a remnant core. Figure 1 shows how certain observed properties of Psyche (discussed below) will be used to test this hypothesis.

Metallic cores in non-impact disrupted planetary bodies are not expected to have been magnetized by any dynamo fields they generate because thermal blanketing by the mantle ensures they always remain above their Curie point during the dynamo's lifetime. However, the exterior of a mantle-stripped planetesimal's core may cool below the Curie point while a dynamo was still being generated by the molten interior (Neufeld et al., 2019). As such,

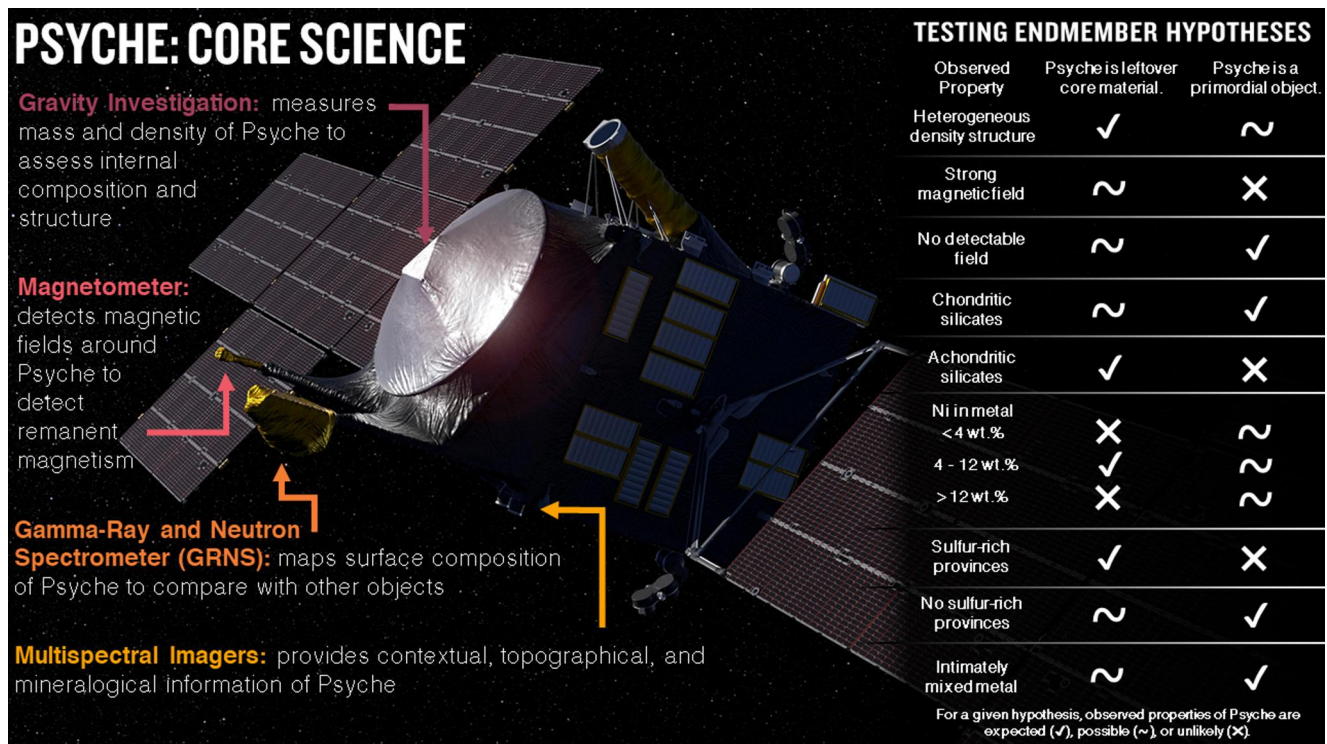


Figure 1. The primary science goal of the Psyche mission is to determine if asteroid (16) Psyche is a planetary core or if it is primordial, unmelted material. The mission will accomplish this using three instrument systems—a Magnetometer, Multispectral Imager, and Gamma-Ray and Neutron Spectrometer—as well as Doppler tracking of the Psyche spacecraft (left). Certain observed properties (right) are expected (✓), possible (~), or unlikely (✗) under the two endmember hypotheses. Background image credit: NASA/JPL-Caltech/ASU.

detection of a strong magnetic dipole moment ($>2 \times 10^{14} \text{ A}\cdot\text{m}^2$) would likely indicate that Psyche once generated a dynamo and thus likely underwent metal-silicate differentiation (Weiss et al., 2023). In particular, if Psyche is uniformly magnetized with an intensity in the range of natural remanent magnetization found in iron meteorites, it would form a present-day magnetosphere even though any early dynamo has long decayed (Oran et al., 2022; Weiss et al., 2023). Such a measurement would likely be the best evidence that Psyche is a planetary core. The Magnetometry Investigation was designed to be able to detect the field of such a dipole moment from orbit in the face of solar wind variations and spacecraft and sensor noise (Elkins-Tanton et al., 2020; Oran et al., 2022; Weiss et al., 2023). Nevertheless, the absence of a measurable magnetic field would not disprove that Psyche is a metal core. Venus, for example, is known to have an iron core but no appreciable magnetic field (Nimmo, 2002). Similarly, the conditions of core cooling and crystallization on Psyche might not have generated the fluid flows required for a dynamo or the surface materials might not have retained a remanent magnetization from an earlier epoch. Discriminating between these two scenarios will require synthesizing information from the other science investigations.

We will also test the core hypothesis using measurements of Psyche's surface composition. Multispectral imaging of the surface will provide resolution well below our requirement of $500 \text{ m}\cdot\text{pixel}^{-1}$ at near-IR wavelengths (725, 850, 948, and 1,025 nm), which will provide information on the silicate fraction, composition, and distribution. Elemental abundances provided by the GRNS will constrain the metal-silicate ratio, the composition of the silicates and their relationship with achondritic and/or chondritic meteorites, and the redox conditions of Psyche's formation. If the abundance of metal is high (e.g., $\geq 30\text{--}50 \text{ vol.}\%$ metal, consistent with remote sensing measurements), it's possible that Psyche represents material from the core of a differentiated protoplanet. If the silicate and metal abundances are similar, and if there is evidence for heterogeneity of surface composition (measured as the variation in reflectance at key wavelengths and/or elemental abundances) on the scale of kilometers, Psyche could perhaps be a mixture of materials generated during a disruptive impact event. Alternatively, if there is $<40 \text{ vol.}\%$ metal and/or a homogeneous distribution of metal and silicates at a submeter scale, then Psyche could be a

primordial, unmelted object similar to chondrites. The Multispectral Imager and GRNS were designed to discriminate between such scenarios. The Imager will determine if there are contiguous silicate regions on scales larger than 1 km² (defined as areas with >14 mol.% Si), while the GRNS will provide precise measurements of the Fe, Si, K, Ni, and either Ca or Al abundances in the top ~1 m of the surface.

In addition, Psyche's bulk and near-surface density constrain its formation. High resolution imaging (~20 m-pixel⁻¹) of >80% of the surface of Psyche enables a precise shape model to be developed (~50 m vertical accuracy globally, compared with multikilometer uncertainty in current shape model dimensions), while radio tracking of the spacecraft motion near Psyche enables determination of the asteroid's mass, gravity field, and internal structure (Jaumann et al., 2022; Zuber et al., 2022). Combining the two provides Psyche's bulk density and local surface density to around degree and order 10, which can be compared with other planetary objects and materials. Second, variation in the surface density measured as the spacecraft orbits can further inform our understanding of Psyche's formation. If Psyche was fully molten, it may have a homogenous surface density (likely modified by subsequent impacts) and radially varying internal structure. Large density variations at depth may indicate Psyche was never molten or is composed of disrupted and reassembled core materials. To address these measurements, the Imager and Gravity Investigations will determine whether Psyche has density variations of ≥25% over a length scale of 50 km.

2.2. Determine the Relative Ages of Regions of Psyche's Surface

Counting the surface density of impact craters can be used to determine the absolute and relative ages of features on planetary surfaces (Bland, 2003). Over time, surfaces accumulate more and larger craters and younger features will generally have fewer craters. Based on past missions to other asteroids and Earth-based observations of Psyche's shape, it is expected that impact craters will be preserved on its surface in varying states of degradation (Russell et al., 2013; Shepard et al., 2021). In addition to better understanding the physics of impacts into metal-rich bodies (e.g., target cratering strength and crater morphology), comparison of the size-frequency distribution of craters on Psyche's surface with main-belt crater chronology will enable estimates of the age of the surface and comparison with the geologic histories of other solar system bodies (Marchi et al., 2020, 2022). To address these questions, high resolution imaging of the surface will be provided by the Multispectral Imager to count craters with diameters larger than 1 km over at least 50% of the surface.

2.3. Determine Whether Small Metal Bodies Incorporate the Same Light Elements Into the Metal Phase as Are Expected in Earth's High Pressure Core

Earth's core has density and seismic velocities almost 10% lower and ~4%–5% higher, respectively, than that predicted by laboratory measurements at relevant temperatures and pressures (e.g., Hirose et al., 2021). Earth's core thus contains substantial amounts of “light elements” with atomic numbers less than that of iron. However, the identities and proportions of these elements are unknown and debated. Historically, popular candidates to explain the density deficit include S, Si, O, C, and H (Hirose et al., 2021).

It is not expected that Earth's core will have the exact same composition as Psyche. Metal that formed Earth's core reacted with mantle silicates at typical pressures >50 GPa and temperatures >3000 K, far more extreme than found inside even the largest asteroids (e.g., Ceres' core at <1500 K and <180 MPa) (Fischer et al., 2015; Neveu et al., 2015; Zolotov, 2020). During the late stages of accretion, however, impactors may have only equilibrated with part of the proto-Earth (e.g., Nakajima et al., 2021). Earth's composition may (at least somewhat) reflect the initial composition of the protoplanets that it ingested. If Psyche is a core, determining its composition would help guide models of Earth's accretion, including by elucidating if what we have measured for metal-rich meteorites is in fact representative of large metal asteroids. To make such comparisons to models of the Earth's core, the Psyche GRNS will determine average abundances of the light elements S, K, and Si in the portions of Psyche's surface that appear to be a metal phase. The GRNS will also be able to measure C and O abundances across Psyche's surface (e.g., Evans et al., 2012; Peplowski et al., 2015). Additionally, H abundance can be inferred from epithermal neutrons measured by the GRNS (e.g., Lawrence et al., 2022). However, the H abundance on Psyche's surface is likely strongly influenced by solar wind implantation, and the abundance of C and H on Psyche's surface have likely been modified by infalling carbonaceous chondritic material. Therefore, they are not included in the required measurement to address this science objective.

2.4. Determine Whether Psyche Was Formed Under Conditions More Oxidizing or More Reducing Than Earth's Core

In addition to composition, temperature, and parent body size, the redox state of an asteroid is key to determining its formation history and comparing it with other solar system objects (McCoy et al., 2022). The redox state of an object can be quantified using oxygen fugacity, an equivalent of the partial pressure of gaseous oxygen in the system corrected for non-ideality of the system. In such a system, the existence of both metal and oxide in relative equilibrium fixes the oxygen fugacity at a certain value (assuming constant temperature and pressure), such that variation in the absolute abundance of metal or oxide does not change the oxygen fugacity (McCoy et al., 2022). Such pairs of metal and oxide [for example, iron (Fe), and wüstite (FeO)] are referred to as buffers. Because some minerals (e.g., iron metal) are only stable at certain oxygen fugacities, the relative abundances of metal and oxide observed in a planetary system can be used to constrain the oxygen fugacity relative to the buffer and therefore allows interpretation of the redox conditions under which an object formed (Bercovici et al., 2022; McCoy et al., 2022).

For example, Mars and some primitive carbonaceous chondrites (e.g., CI, CM, CK, CO, and CV) are thought to be relatively more oxidized compared to Mercury, Earth, and metal-rich meteorites (e.g., EH, CB, and H chondrites) (McCoy et al., 2022). The detection of any endogenous iron metal on the surface of Psyche would constrain the redox conditions of its formation to be at or below those of the iron-wüstite buffer, indicating reducing conditions. Further constraints can be obtained by measuring the abundance of certain elements (e.g., Ni in the iron metal), identification of key sulfide phases (e.g., oldhamite, CaS), and possibly the ratio of FeO in silicates to Fe in metal (Elkins-Tanton et al., 2022; McCoy et al., 2022). High (>10–12 wt.%) concentrations of Ni in iron metal would indicate that Psyche experienced conditions oxidizing enough to transform significant Fe into FeO, leaving behind Ni. This abundance in Ni could be detected by GRNS and the variation of FeO in silicates would be detectable by the Multispectral Imager. Finally, sulfide minerals such as oldhamite and troilite (FeS) exhibit changes in spectral slope at visible wavelengths that can be characterized by multispectral data (Dibb et al., 2023). To accomplish this objective, the Psyche mission will determine whether Psyche's surface has a global average of >10 wt.% oldhamite and <4 wt.% Ni (indicating reducing conditions) or >12 wt.% Ni (indicating oxidizing conditions) using the Multispectral Imager and GRNS.

2.5. Characterize Psyche's Morphology

The most recent shape model for Psyche (Shepard et al., 2021) indicates that Psyche has several depressions, likely large craters that hint to a violent impact history akin to asteroids Vesta and Pallas (e.g., Marsset et al., 2020; Schenk et al., 2012). Beyond the observed depressions, the possible topography of a metal-rich asteroid is largely unknown. It is plausible that impact craters may be deeper and have sharper rims than previously seen on rocky asteroids: Marchi et al. (2020) conducted hypervelocity impact experiments into metal targets and measured a mean depth-to-diameter ratio of craters in those targets of 0.41 ± 0.01 , compared to a depth-to-diameter ratio of 0.15–0.25 for craters in rocky targets. Second, a wide diversity of crater morphologies may exist depending on the local abundance of iron and its proximity to the surface (Marchi et al., 2020, 2022; Raducan et al., 2020). Detection of crater degradation or erasure may hint at seismic shaking events from subsequent impacts (e.g., Baijal et al., 2023). Global contraction and subsequent cracking of a cooling metal body may lead to scarps on the order of 10 km tall on Psyche's surface (Elkins-Tanton et al., 2020; Jaumann et al., 2022).

Furthermore, models of core formation and remote sensing data suggest that ferrovulcanic eruptions and/or erosional impacts may have emplaced and exposed vast reservoirs of nearly pure metal on Psyche's surface (Abrahams & Nimmo, 2019; Cambioni et al., 2022; Johnson et al., 2020; Shepard et al., 2021). Models of core formation from different meteorite groups suggest that the sulfur content of parent metal cores may exceed 5 wt. %, enough to form an immiscible sulfide liquid that could be exposed when Psyche was potentially stripped of its mantle (Bercovici et al., 2022; Chabot, 2004). Some telescopic spectra of Psyche are indeed consistent with spectra of sulfide minerals, like troilite and pentlandite $[(\text{Fe,Ni})_9\text{S}_8]$ (Dibb et al., 2023). The physical, mineralogical, and spectral consequences of the exposure to space of such materials are still being explored at the laboratory scale (e.g., Christoph et al., 2022; Matsumoto et al., 2021).

High spatial resolution imaging of Psyche's surface from multiple viewing angles (between 15 and 90° stereo separation) and under different lighting conditions (solar phase angles between 0 and 90°) will be used to generate digital terrain models (DTMs) of the surface (Jaumann et al., 2022). Orbit B has been designed to characterize

Psyche's morphology over 50% of its surface at 200 m-pixel^{-1} horizontal pixel scale and 50 m vertical height accuracy, capturing Psyche's topography and enabling geologic mapping. The Imager was designed to meet this requirement and the mission will address this objective following the conclusion of both parts of Orbit B.

3. The Psyche Mission and Spacecraft Payload

The Psyche mission is composed of the Psyche spacecraft and the Earth-based infrastructure necessary to build, launch, and support a space mission throughout its lifetime. Psyche contributes to NASA's Science Mission Directorate's Priority Goals for Science in 2020–2024 and is aligned with other community goals documents (e.g., the Small Bodies Assessment Group 2020 Goals Document). The Psyche mission leverages significant heritage from previous missions and is a logical follow-on to the Dawn mission to the asteroids (1) Ceres and (4) Vesta (Oh et al., 2016; Polanskey et al., 2016). The mission will deliver key science by studying the asteroid through four complementary investigations over 26 months beginning in August 2029. Here we offer a brief description of each of the four investigations.

3.1. The Magnetometer

The Magnetometer is composed of two three-axis fluxgate Sensor Units mounted 0.7 m apart along a 2.15-m long boom and connected to two Electronics Units located within the spacecraft bus (Weiss et al., 2023). This configuration provides redundancy and allows for removal of magnetic field contributions from the spacecraft to detect fields from any remanent magnetization. The Magnetometer samples at up to 50 Hz, has a range of $\pm 80,000 \text{ nT}$, and an instrument noise of 39 pT axis^{-1} (3σ) integrated over 0.1–1 Hz. The Magnetometer will be powered on shortly after launch and will collect data throughout the entire mission (Weiss et al., 2023).

3.2. The Multispectral Imager

The Multispectral Imager is a block-redundant pair of digital charge coupled device cameras with 148-mm focal length optics that will obtain polychromatic and narrow-band color images of the asteroid at pixel scales ranging from 35 down to $\sim 3.8 \text{ m-pixel}^{-1}$ (assuming nominally planned orbital altitudes) (Bell et al., 2016; Dobb et al., 2023). The Imager will observe the surface through a nadir-pointing, broadband clear filter, through seven color filters across the 427–1,025 nm wavelength region optimized to identify silicate and sulfide minerals, and through the clear filter at multiple look angles to produce DTMs using image-based stereo photogrammetry or stereo photoclinometry. The Imagers will also be used for optical navigation during the mission's cruise to Psyche and to provide geologic context for measurements made by the other instruments.

3.3. The Gamma-Ray and Neutron Spectrometer

The Gamma-Ray and Neutron Spectrometer (GRNS) will quantify Psyche's abundances for the elements Ni, Fe, Si, K, S, Al, and Ca, as well as the spatial distribution of Psyche's metal-to-silicate fraction (or metal fraction) (Peplowski et al., 2022). The Gamma-Ray Spectrometer (GRS) uses a high-purity Ge (HPGe) sensor to detect cosmic-ray generated gamma-rays in the 0.1- to 10-MeV energy range. The outer housing of the GRS contains a borated plastic anticoincidence shield (ACS) that provides three functions: active background rejection from charged particle interactions in the HPGe sensor; fast neutron measurements; and direct measurements of the incident galactic cosmic ray flux. The Neutron Spectrometer (NS) uses three ^3He gas proportional sensors, each with different material wraps that serve as neutron energy filters. The neutron energy ranges measured by the NS are thermal ($<0.3 \text{ keV}$), low-energy epithermal (0.3 eV–1 keV), and high-energy epithermal (up to 100 keV).

3.4. The Gravity Investigation

The Psyche spacecraft is equipped with a 2-m high-gain antenna and three low-gain antennae and will use X-band frequencies to provide uplink and downlink (Zuber et al., 2022). Spacecraft tracking will be provided by NASA's Deep Space Network. The Gravity Investigation will measure the gravitational field of Psyche, primarily by the analysis of the Doppler shift of spacecraft emitted radio signals from the three low-gain antennae (Zuber et al., 2022). The accuracy of the recovered gravity field is dictated by the X-band system performance, which is expected to be of the order 0.1 mm-s^{-1} at 60-s integration time. This experiment will provide a much better measurement of the asteroid's mass (uncertainty on GM reduced to $<0.001 \text{ km}^3 \text{ s}^{-2}$ for gravitational constant, G , and Psyche's mass, M) and therefore bulk density. Furthermore, a spherical harmonic model of gravity to degree

and order 10 will be produced, enabling quantification of the asteroid's subsurface density distribution at an effective resolution approximately equal to the spacecraft's lowest planned orbital altitude (~ 75 km) (Zuber et al., 2022).

4. Additional Value of the Psyche Mission

Experience shows that all space missions bring both surprises in observations and inspiration for additional theoretical or experimental work. While the following is unfunded and explicitly not required to achieve mission success, here we discuss additional questions that may benefit from data collected during the Psyche mission.

4.1. Regolith Formation and Evolution on Metal-Rich Bodies

On airless planetary bodies, impacts and thermal fatigue produce unconsolidated materials (regolith) from comminution of existing surface materials (e.g., Ballouz et al., 2020; Cambioni et al., 2021). Laboratory experiments indicate that cratering in iron-nickel meteorites and ingots can produce small metal fragments resembling rocky regolith (Christoph et al., 2021; Marchi et al., 2020). Moreover, Psyche's large obliquity (95°) and moderately high eccentricity (0.134) may lead to large thermal variations which can cause cracking of metallic boulders (Bierson et al., 2022). However, remote-sensing data suggest that Psyche's upper meter consists of a porous unconsolidated mixture of metal-rich and silicate materials (Cambioni et al., 2022; de Kleer et al., 2021; Landsman et al., 2018; Matter et al., 2013; Shepard et al., 2021). Do large metal blocks, which may be present on Psyche, comminute at a similar rate to silicates? Does the brittle-to-ductile temperature transition of metals play a role in regolith formation? Do landforms composed of such materials evolve similarly to comparable features on other terrestrial bodies?

Furthermore, regoliths on the Moon and stony asteroids exhibit reflectance spectra that are redder, darker, and have lower spectral contrast (i.e., shallower absorption features) than their constituent minerals do in laboratory measurements, a result of weathering by both solar wind ions and micrometeoroid bombardment (Adams & McCord, 1971; Chapman, 2004; Chapman & Salisbury, 1973; Pieters et al., 2000). The production of nanophase iron particles is often invoked to explain these spectral trends, but does a surface already rich in metal experience different spectral trends? Second, if Psyche does have extensive sulfur-rich areas on the surface, how do those materials mature?

4.2. Dynamical Constraints and Connections to Other Metal-Rich Bodies

Psyche will be the largest asteroid ever visited in the 100–500 km diameter size range, which could mark the transition between bodies that are too large to be destroyed in collisions and those that are instead the fragments of catastrophic collisions (Ceres and Vesta, with diameters larger than 500 km, could represent objects too large to be catastrophically disrupted as may have happened for Psyche) (e.g., Bottke et al., 2005; Marchi et al., 2022). Large M-types have main-belt orbits that suggest that they interacted with ancient mean motion resonances of Jupiter (i.e., resonances that existed before Jupiter's final migration phase; Scott et al., 2015). If true, the M-types likely interacted with these resonances when Jupiter was near its full size and the resonances had their maximum power. However, it is still not known whether M-type asteroids formed in the inner or outer solar system (Elkins-Tanton et al., 2022). This story becomes more intriguing if the M-types are linked to metal-rich CB chondrites (e.g., Dobb et al., 2023). These meteorites have the youngest measured chondrules and it has been suggested that CBs formed from late-stage protoplanetary collisions when the solar nebula was presumably close to dissipation and Jupiter was near its full size (Krot et al., 2005). Taken together, this may point to Psyche and the M-types as some of the last objects captured during early giant planet migration. Generally, in what ways is Psyche a representative of the M/X-type asteroids, and in what ways can data from Psyche further our understanding of primitive, metal-rich meteorites?

The only other M-type asteroid visited by spacecraft, (21) Lutetia, offers other points of comparison with data from Psyche. The bulk density of Lutetia as measured during the flyby of the Rosetta spacecraft was $3,400 \pm 300 \text{ kg}\cdot\text{m}^{-3}$, which, with an assumed macroporosity of 12%, was interpreted to indicate an abundance of high atomic number elements (e.g., iron) throughout the body (Pätzold et al., 2011). However, its surface was composed of a lunar-like powdery regolith consistent with unaltered low-Fe silicates (Coradini et al., 2011). These two contrasting observations indicate that Lutetia may be only partially differentiated and therefore may offer additional context to measurements from Psyche (Weiss et al., 2012). Is Psyche representative of material

from a more differentiated body than Lutetia? Do the two objects capture different snapshots along a general evolutionary timeline for small bodies?

4.3. Characterizing the Space Weather and Cosmic Gamma-Ray Environments

The GRNS offers the opportunity to carry out additional measurements beyond quantifying the elemental composition of Psyche's surface. Most importantly, the NS and GRS ACS are planned to be operated during most of the mission's cruise phase to collect data for background calibrations. These sensors are sensitive to energetic charged particles greater than tens of MeV and thus enable a characterization of the charged particle and space weather environment throughout the mission. How can measurements from the Psyche spacecraft supplement previous studies of heliospheric structure and particle transport in the inner solar system (e.g., Lawrence et al., 2016)? One other phenomenon of interest is gamma ray bursts, which are highly energetic signatures of the deaths of massive stars and compact object mergers (Luongo & Muccino, 2021). The GRS ACS is also sensitive to gamma-rays and is configured with an autonomous gamma ray burst monitor. This enables the ACS to be one node in an interplanetary network of monitors that uses triangulation to constrain the location and timing of cosmic gamma ray bursts (Hurley et al., 2013).

5. Conclusions

Observations of (16) Psyche from Earth indicate it to be a metal-rich object. The Psyche mission is designed to test hypotheses of the formation of the asteroid and compare it with other metal-rich objects by addressing five primary science objectives. The Psyche mission will accomplish this by detailed mapping of the asteroid's surface composition, measuring its shape and interior structure, and characterizing any magnetic field present. The Psyche spacecraft was successfully launched in October 2023 and has now begun its cruise phase to the asteroid. A flyby of Mars will provide an opportunity to collect valuable calibration data before the spacecraft reaches the asteroid in August 2029. Data collected from the mission will be made publicly available on NASA's Planetary Data System and displayed on the mission's website (<https://psyche.asu.edu>), encouraging the public to follow along with this exciting mission as we learn what Psyche is, how it formed, and what it can tell us about our home planet.

Conflict of Interest

The authors declare no conflicts of interest relevant to this study.

Data Availability Statement

This work uses no new samples or data.

Acknowledgments

The authors are extremely grateful to the entire Psyche Team for their dedication and hard work in building and executing this mission. This work is supported by NASA contract NNM16AA09, "Psyche: Journey to a Metal World." S. Cambioni acknowledges funding from the Crosby Distinguished Postdoctoral Fellowship Program of the Department of Earth, Atmospheric and Planetary Science, Massachusetts Institute of Technology and from NASA contract NNM16AA09, "Psyche: Journey to a Metal World." M. Wiczeorek acknowledges funding from the French space agency, CNES. E. Asphaug acknowledges support from NASA contract NNM16AA09, "Psyche: Journey to a Metal World" and from U. Arizona Research, Innovation, and Impact.

References

- Abrahams, J. N., & Nimmo, F. (2019). Ferrovulcanism: Iron volcanism on metallic asteroids. *Geophysical Research Letters*, 46(10), 5055–5064. <https://doi.org/10.1029/2019gl082542>
- Adams, J. B., & McCord, T. B. (1971). Alteration of lunar optical properties: Age and composition effects. *Science*, 171(3971), 567–571. <https://doi.org/10.1126/science.171.3971.567>
- Adibekyan, V., Dorn, C., Sousa, S. G., Santos, N. C., Bitsch, B., Israelian, G., et al. (2021). A compositional link between rocky exoplanets and their host stars. *Science*, 374(6565), 330–332. <https://doi.org/10.1126/science.abg8794>
- Aguichine, A., Mousis, O., Devouard, B., & Ronnet, T. (2020). Rocklines as cradles for refractory solids in the protosolar nebula. *The Astrophysical Journal*, 901(2), 97. <https://doi.org/10.3847/1538-4357/abaf47>
- Asphaug, E., & Reufer, A. (2014). Mercury and other iron-rich planetary bodies as relics of inefficient accretion. *Nature Geoscience*, 7(8), 564–568. <https://doi.org/10.1038/ngeo2189>
- Bajjal, N., Denton, C., & Asphaug, E. (2023). Seismic transmission through asteroid interiors: Insights from impact models. In *Asteroid, Comets, Meteorites Conference abstract. # 2851*. Retrieved from <https://www.hou.usra.edu/meetings/acm2023/pdf/2218.pdf>
- Ballouz, R. L., Walsh, K. J., Barnouin, O. S., DellaGiustina, D. N., Asad, M. A., Jawin, E. R., et al. (2020). Bennu's near-Earth lifetime of 1.75 million years inferred from craters on its boulders. *Nature*, 587(7833), 205–209. <https://doi.org/10.1038/s41586-020-2846-z>
- Bass, J. D. (1995). Elasticity of minerals, glasses, and melts. *Mineral physics and crystallography: A handbook of physical constants* (Vol. 2, pp. 45–63).
- Becker, T. M., Cunningham, N., Molyneux, P., Roth, L., Feaga, L. M., Retherford, K. D., et al. (2020). HST UV observations of asteroid (16) Psyche. *The Planetary Science Journal*, 1(3), 53. <https://doi.org/10.3847/PSJ/abb67e>
- Bell, III, J. F., Elkins-Tanton, L. T., Polanskey, C. A., Ravine, M. A., Caplinger, M. A., Asphaug, E., et al. (2016). The Psyche Multispectral Imager investigation: Characterizing the geology, topography, and compositional properties of a metallic world (Vol. 47, No. 1366).
- Bercovici, H. L., Elkins-Tanton, L. T., O'Rourke, J. G., & Schaefer, L. (2022). The effects of bulk composition on planetesimal core sulfur content and size. *Icarus*, 380, 114976. <https://doi.org/10.1016/j.icarus.2022.114976>

- Bierson, C. J., Elkins-Tanton, L. T., & O'Rourke, J. G. (2022). Thermal fatigue on 16 Psyche driven by a combination of high obliquity and surface composition. In *AGU Fall Meeting Abstracts* (Vol. 2022, p. P25D-2138).
- Binzel, R. P., Bus, S. J., Xu, S., Sunshine, J., Burbine, T. H., Neely, A. W., & Brown, R. W. (1995). Rotationally resolved spectra of asteroid 16 Psyche. *Icarus*, 117(2), 443–445. <https://doi.org/10.1006/icar.1995.1170>
- Bland, P. (2003). Crater counting. *Astronomy & Geophysics*, 44(4), 4–21. <https://doi.org/10.1046/j.1468-4004.2003.44421.x>
- Bottke, W. F., Jr., Durda, D. D., Nesvorný, D., Jedicke, R., Morbidelli, A., Vokrouhlický, D., & Levison, H. (2005). The fossilized size distribution of the main asteroid belt. *Icarus*, 175(1), 111–140. <https://doi.org/10.1016/j.icarus.2004.10.026>
- Burbine, T. H., & Binzel, R. P. (2002). Small main-belt asteroid spectroscopic survey in the near-infrared. *Icarus*, 159(2), 468–499. <https://doi.org/10.1006/icar.2002.6902>
- Burbine, T. H., Meibom, A., & Binzel, R. P. (1996). Mantle material in the main belt: Battered to bits? *Meteoritics & Planetary Science*, 31(5), 607–620. <https://doi.org/10.1111/j.1945-5100.1996.tb02033.x>
- Bus, S. J., & Binzel, R. P. (2002). Phase II of the small main-belt asteroid spectroscopic survey: A feature-based taxonomy. *Icarus*, 158(1), 146–177. <https://doi.org/10.1006/icar.2002.6856>
- Cambioni, S., de Kleer, K., & Shepard, M. (2022). The heterogeneous surface of asteroid (16) Psyche. *Journal of Geophysical Research: Planets*, 127(6), e2021JE007091. <https://doi.org/10.1029/2021je007091>
- Cambioni, S., Delbo, M., Poggiali, G., Avdellidou, C., Ryan, A. J., Deshapriya, J. D. P., et al. (2021). Fine-regolith production on asteroids controlled by rock porosity. *Nature*, 598(7879), 49–52. <https://doi.org/10.1038/s41586-021-03816-5>
- Carry, B. (2012). Density of asteroids. *Planetary and Space Science*, 73(1), 98–118. <https://doi.org/10.1016/j.pss.2012.03.009>
- Chabot, N. L. (2004). Sulfur contents of the parental metallic cores of magmatic iron meteorites. *Geochimica et Cosmochimica Acta*, 68(17), 3607–3618. <https://doi.org/10.1016/j.gca.2004.03.023>
- Chapman, C. R. (2004). Space weathering of asteroid surfaces. *Annual Review of Earth and Planetary Sciences*, 32(1), 539–567. <https://doi.org/10.1146/annurev.earth.32.101802.120453>
- Chapman, C. R., & Salisbury, J. W. (1973). Comparisons of meteorite and asteroid spectral reflectivities. *Icarus*, 19(4), 507–522. [https://doi.org/10.1016/0019-1035\(73\)90078-x](https://doi.org/10.1016/0019-1035(73)90078-x)
- Christoph, J. M., Minesinger, G. M., Bu, C., Dukes, C. A., & Elkins-Tanton, L. T. (2022). Space weathering effects in troilite by simulated solar-wind hydrogen and helium ion irradiation. *Journal of Geophysical Research: Planets*, 127(5), e2021JE006916. <https://doi.org/10.1029/2021je006916>
- Christoph, J. M., Sharp, T., Marchi, S., & Elkins-Tanton, L. T. (2021). Characterizing ejecta fragments from impact experiments into meteoric iron using scanning electron microscopy (SEM). In *Paper presented at 52nd Lunar and Planetary Science Conference, abstract #2730*.
- Coradini, A., Capaccioni, F., Erard, S., Arnold, G., De Sanctis, M. C., Filacchione, G., et al. (2011). The surface composition and temperature of asteroid 21 Lutetia as observed by Rosetta/VIRTIS. *Science*, 334(6055), 492–494. <https://doi.org/10.1126/science.1204062>
- de Gasparis, A. (1893). Annibale de Gasparis. *Monthly Notices of the Royal Astronomical Society*, 53(4), 225–226. <https://doi.org/10.1093/mnras/53.4.225>
- de Kleer, K., Cambioni, S., & Shepard, M. (2021). The surface of (16) Psyche from thermal emission and polarization mapping. *The Planetary Science Journal*, 2(4), 149. <https://doi.org/10.3847/psj/ac01ec>
- DeMeo, F. E., Binzel, R. P., Slivan, S. M., & Bus, S. J. (2009). An extension of the Bus asteroid taxonomy into the near-infrared. *Icarus*, 202(1), 160–180. <https://doi.org/10.1016/j.icarus.2009.02.005>
- Dibb, S. D., Bell, III, J. F., Elkins-Tanton, L. T., & Williams, D. A. (2023). Visible to near-infrared reflectance spectroscopy of asteroid (16) Psyche: Implications for the Psyche mission's science investigations. *Earth and Space Science*, 10(1), e2022EA002694. <https://doi.org/10.1029/2022ea002694>
- Ebel, D. S., & Stewart, S. T. (2018). The elusive origin of Mercury. *Mercury: The View after MESSENGER* (pp. 497–515).
- Elkins-Tanton, L. T., Asphaug, E., Bell, J. F., III, Bercovici, H., Bills, B., Binzel, R., et al. (2020). Observations, meteorites, and models: A preflight assessment of the composition and formation of (16) Psyche. *Journal of Geophysical Research: Planets*, 125(3), e2019JE006296. <https://doi.org/10.1029/2019je006296>
- Elkins-Tanton, L. T., Asphaug, E., Bell, J. F., III, Bierson, C. J., Bills, B. G., Bottke, W. F., et al. (2022). Distinguishing the origin of asteroid (16) Psyche. *Space Science Reviews*, 218(3), 17. <https://doi.org/10.1007/s11214-022-00880-9>
- Evans, L. G., Peplowski, P. N., Rhodes, E. A., Lawrence, D. J., McCoy, T. J., Nittler, L. R., et al. (2012). Major-element abundances on the surface of Mercury: Results from the MESSENGER Gamma-Ray Spectrometer. *Journal of Geophysical Research*, 117(E12), E00L07. <https://doi.org/10.1029/2012je004178>
- Fischer, R. A., Nakajima, Y., Campbell, A. J., Frost, D. J., Harries, D., Langenhorst, F., et al. (2015). High pressure metal–silicate partitioning of Ni, Co, V, Cr, Si, and O. *Geochimica et Cosmochimica Acta*, 167, 177–194. <https://doi.org/10.1016/j.gca.2015.06.026>
- Fornasier, S., Clark, B. E., Dotto, E., Migliorini, A., Ockert-Bell, M., & Barucci, M. A. (2010). Spectroscopic survey of M-type asteroids. *Icarus*, 210(2), 655–673. <https://doi.org/10.1016/j.icarus.2010.07.001>
- Gabriel, T. S., & Cambioni, S. (2023). The role of giant impacts in planet formation. *Annual Review of Earth and Planetary Sciences*, 51(1), 671–695. <https://doi.org/10.1146/annurev-earth-031621-055545>
- Garvie, L. A., Knauth, L. P., & Morris, M. A. (2017). Sedimentary laminations in the Isheyevo (CH/CBb) carbonaceous chondrite formed by gentle impact-plume sweep-up. *Icarus*, 292, 36–47. <https://doi.org/10.1016/j.icarus.2017.03.021>
- Hardersen, P. S., Gaffey, M. J., & Abell, P. A. (2005). Near-IR spectral evidence for the presence of iron-poor orthopyroxenes on the surfaces of six M-type asteroids. *Icarus*, 175(1), 141–158. <https://doi.org/10.1016/j.icarus.2004.10.017>
- Hirose, K., Wood, B., & Vočadlo, L. (2021). Light elements in the Earth's core. *Nature Reviews Earth & Environment*, 2(9), 645–658. <https://doi.org/10.1038/s43017-021-00203-6>
- Hurley, K., Pal'Shin, V. D., Aptekar, R. L., Golenetskii, S. V., Frederiks, D. D., Mazets, E. P., et al. (2013). The interplanetary network supplement to the Fermi GBM catalog of cosmic gamma-ray bursts. *The Astrophysical Journal Supplement Series*, 207(2), 39. <https://doi.org/10.1088/0067-0049/207/2/39>
- Jaumann, R., Bell, III, J. F., Polanskey, C. A., Raymond, C. A., Asphaug, E., Bercovici, D., et al. (2022). The Psyche topography and geomorphology investigation. *Space Science Reviews*, 218(2), 7. <https://doi.org/10.1007/s11214-022-00874-7>
- Johnson, B. C., Sori, M. M., & Evans, A. J. (2020). Ferrovulcanism on metal worlds and the origin of pallasites. *Nature Astronomy*, 4(1), 41–44. <https://doi.org/10.1038/s41550-019-0885-x>
- Johnson, B. C., Walsh, K. J., Minton, D. A., Krot, A. N., & Levison, H. F. (2016). Timing of the formation and migration of giant planets as constrained by CB chondrites. *Science Advances*, 2(12), e1601658. <https://doi.org/10.1126/sciadv.1601658>
- Krot, A. N., Amelin, Y., Cassen, P., & Meibom, A. (2005). Young chondrules in CB chondrites from a giant impact in the early Solar System. *Nature*, 436(7053), 989–992. <https://doi.org/10.1038/nature03830>

- Krot, A. N., Keil, K., Scott, E. R. D., Goodrich, C. A., & Weisberg, M. K. (2014). Classification of meteorites and their genetic relationships. *Treatise on Geochemistry* (2nd ed., pp. 1–63).
- Kruijer, T. S., Burkhardt, C., Budde, G., & Kleine, T. (2017). Age of Jupiter inferred from the distinct genetics and formation times of meteorites. *Proceedings of the National Academy of Sciences*, 114(26), 6712–6716. <https://doi.org/10.1073/pnas.1704461114>
- Kruijer, T. S., Kleine, T., & Borg, L. E. (2020). The great isotopic dichotomy of the early Solar System. *Nature Astronomy*, 4(1), 32–40. <https://doi.org/10.1038/s41550-019-0959-9>
- Landsman, Z. A., Emery, J. P., Campins, H., Hanuš, J., Lim, L. F., & Cruikshank, D. P. (2018). Asteroid (16) Psyche: Evidence for a silicate regolith from spitzer space telescope spectroscopy. *Icarus*, 304, 58–73. <https://doi.org/10.1016/j.icarus.2017.11.035>
- Lawrence, D. J., Peplowski, P. N., Feldman, W. C., Schwadron, N. A., & Spence, H. E. (2016). Galactic cosmic ray variations in the inner heliosphere from solar distances less than 0.5 AU: Measurements from the MESSENGER Neutron Spectrometer. *Journal of Geophysical Research: Space Physics*, 121(8), 7398–7406. <https://doi.org/10.1002/2016ja022962>
- Lawrence, D. J., Peplowski, P. N., Wilson, J. T., & Elphic, R. C. (2022). Global hydrogen abundances on the lunar surface. *Journal of Geophysical Research: Planets*, 127(7), e2022JE007197. <https://doi.org/10.1029/2022je007197>
- Luongo, O., & Muccino, M. (2021). A roadmap to gamma-ray bursts: New developments and applications to cosmology. *Galaxies*, 9(4), 77. <https://doi.org/10.3390/galaxies9040077>
- Magri, C., Nolan, M. C., Ostro, S. J., & Giorgini, J. D. (2007). A radar survey of main-belt asteroids: Arecibo observations of 55 objects during 1999–2003. *Icarus*, 186(1), 126–151. <https://doi.org/10.1016/j.icarus.2006.08.018>
- Marchi, S., Asphaug, E., Bell, III, J. F., Bottke, W. F., Jaumann, R., Park, R. S., et al. (2022). Determining the relative cratering ages of regions of Psyche's surface. *Space Science Reviews*, 218(4), 24. <https://doi.org/10.1007/s11214-022-00891-6>
- Marchi, S., Durda, D. D., Polanskey, C. A., Asphaug, E., Bottke, W. F., Elkins-Tanton, L. T., et al. (2020). Hypervelocity impact experiments in iron-nickel ingots and iron meteorites: Implications for the NASA Psyche mission. *Journal of Geophysical Research: Planets*, 125(2), e2019JE005927. <https://doi.org/10.1029/2019je005927>
- Marsset, M., Brož, M., Vernazza, P., Drouard, A., Castillo-Rogez, J., Hanuš, J., et al. (2020). The violent collisional history of aqueously evolved (2) Pallas. *Nature Astronomy*, 4(6), 569–576. <https://doi.org/10.1038/s41550-019-1007-5>
- Matsumoto, T., Noguchi, T., Tobimatsu, Y., Harries, D., Langenhorst, F., Miyake, A., & Hidaka, H. (2021). Space weathering of iron sulfides in the lunar surface environment. *Geochimica et Cosmochimica Acta*, 299, 69–84. <https://doi.org/10.1016/j.gca.2021.02.013>
- Matter, A., Delbo, M., Carry, B., & Ligor, S. (2013). Evidence of a metal-rich surface for the Asteroid (16) Psyche from interferometric observations in the thermal infrared. *Icarus*, 226(1), 419–427. <https://doi.org/10.1016/j.icarus.2013.06.004>
- McCoy, T. J., Dobb, S. D., Peplowski, P. N., Maurel, C., Bercovici, H. L., Corrigan, C. M., et al. (2022). Deciphering redox state for a metal-rich world. *Space Science Reviews*, 218(2), 6. <https://doi.org/10.1007/s11214-022-00872-9>
- Nakajima, M., Golabek, G. J., Wünnemann, K., Rubie, D. C., Burger, C., Melosh, H. J., et al. (2021). Scaling laws for the geometry of an impact-induced magma ocean. *Earth and Planetary Science Letters*, 568, 116983. <https://doi.org/10.1016/j.epsl.2021.116983>
- Neufeld, J. A., Bryson, J. F. J., & Nimmo, F. (2019). The top-down solidification of iron asteroids driving dynamo evolution. *Journal of Geophysical Research: Planets*, 124(5), 1331–1356. <https://doi.org/10.1029/2018je005900>
- Neveu, M., Desch, S. J., & Castillo-Rogez, J. C. (2015). Core cracking and hydrothermal circulation can profoundly affect Ceres' geophysical evolution. *Journal of Geophysical Research: Planets*, 120(2), 123–154. <https://doi.org/10.1002/2014je004714>
- Nimmo, F. (2002). Why does Venus lack a magnetic field? *Geology*, 30(11), 987–990. [https://doi.org/10.1130/0091-7613\(2002\)030<0987:wvdlam>2.0.co;2](https://doi.org/10.1130/0091-7613(2002)030<0987:wvdlam>2.0.co;2)
- O'Brien, D. P., & Greenberg, R. (2003). Steady-state size distributions for collisional populations: Analytical solution with size-dependent strength. *Icarus*, 164(2), 334–345. [https://doi.org/10.1016/s0019-1035\(03\)00145-3](https://doi.org/10.1016/s0019-1035(03)00145-3)
- Ockert-Bell, M. E., Clark, B. E., Shepard, M. K., Isaacs, R. A., Cloutis, E. A., Fornasier, S., & Bus, S. J. (2010). The composition of M-type asteroids: Synthesis of spectroscopic and radar observations. *Icarus*, 210(2), 674–692. <https://doi.org/10.1016/j.icarus.2010.08.002>
- Oh, D. Y., Goebel, D. M., Elkins-Tanton, L., Polanskey, C., Lord, P., Tilley, S., et al. (2016). Psyche: Journey to a metal world. In *52nd AIAA/SAE/ASEE Joint Propulsion Conference* (p. 4541).
- Oran, R., Weiss, B. P., De Soria Santacruz-Pich, M., Jun, I., Lawrence, D. J., Polanskey, C. A., et al. (2022). Maximum energies of trapped particles around magnetized planets and small bodies. *Geophysical Research Letters*, 49(13), e2021GL097014. <https://doi.org/10.1029/2021GL097014>
- Ostro, S. J., Campbell, D. B., & Shapiro, I. I. (1985). Mainbelt asteroids: Dual-polarization radar observations. *Science*, 229(4712), 442–446. <https://doi.org/10.1126/science.229.4712.442>
- Pätzold, M., Andert, T. P., Asmar, S. W., Anderson, J. D., Barriot, J. P., Bird, M. K., et al. (2011). Asteroid 21 Lutetia: Low mass, high density. *Science*, 334(6055), 491–492. <https://doi.org/10.1126/science.1209389>
- Peplowski, P. N., Goldsten, J. O., Burks, M. T., Lawrence, D. J., Arthur, P. A., Colley, C. N., et al. (2022). The Psyche Gamma-Ray and Neutron Spectrometer: Calibrated, delivered, and ready for launch. In *52nd Lunar and Planetary Science Conference, abstract #2516*.
- Peplowski, P. N., Lawrence, D. J., Evans, L. G., Klima, R. L., Blewett, D. T., Goldsten, J. O., et al. (2015). Constraints on the abundance of carbon in near-surface materials on Mercury: Results from the MESSENGER Gamma-Ray Spectrometer. *Planetary and Space Science*, 108, 98–107. <https://doi.org/10.1016/j.pss.2015.01.008>
- Pieters, C. M., Taylor, L. A., Noble, S. K., Keller, L. P., Hapke, B., Morris, R. V., et al. (2000). Space weathering on airless bodies: Resolving a mystery with lunar samples. *Meteoritics & Planetary Science*, 35(5), 1101–1107. <https://doi.org/10.1111/j.1945-5100.2000.tb01496.x>
- Polanskey, C. A., Joy, S. P., Raymond, C. A., & Rayman, M. D. (2016). Dawn Ceres mission: Science operations performance. In *14th International Conference on Space Operations* (p. 2442).
- Racero, E., Giordano, F., Carry, B., Berthier, J., Müller, T., Mahlke, M., et al. (2022). ESAsky SSOSS: Solar System Object Search Service and the case of Psyche. *Astronomy & Astrophysics*, 659, A38. <https://doi.org/10.1051/0004-6361/202140899>
- Raducan, S. D., Davison, T. M., & Collins, G. S. (2020). Morphological diversity of impact craters on asteroid (16) Psyche: Insight from numerical models. *Journal of Geophysical Research: Planets*, 125(9), e2020JE006466. <https://doi.org/10.1029/2020je006466>
- Rivkin, A. S., Howell, E. S., Britt, D. T., Lebofsky, L. A., Nolan, M. C., & Brannon, D. D. (1995). 3-μm spectrophotometric survey of M- and E-class asteroids. *Icarus*, 117(1), 90–100. <https://doi.org/10.1006/icar.1995.1144>
- Rivkin, A. S., Howell, E. S., Lebofsky, L. A., Clark, B. E., & Britt, D. T. (2000). The nature of M-class asteroids from 3-μm observations. *Icarus*, 145(2), 351–368. <https://doi.org/10.1006/icar.2000.6354>
- Russell, C. T., Raymond, C. A., Jaumann, R., McSweeney, H. Y., De Sanctis, M. C., Nathues, A., et al. (2013). Dawn completes its mission at 4 Vesta. *Meteoritics & Planetary Science*, 48(11), 2076–2089. <https://doi.org/10.1111/maps.12091>
- Sanchez, J. A., Reddy, V., Shepard, M. K., Thomas, C., Cloutis, E. A., Takir, D., et al. (2017). Detection of rotational spectral variation on the M-type asteroid (16) Psyche. *The Astronomical Journal*, 153(1), 29. <https://doi.org/10.3847/1538-3881/153/1/29>

- Schenk, P., O'Brien, D. P., Marchi, S., Gaskell, R., Preusker, F., Roatsch, T., et al. (2012). The geologically recent giant impact basins at Vesta's south pole. *Science*, 336(6082), 694–697. <https://doi.org/10.1126/science.1223272>
- Schmadel, L. D. (2012). *Dictionary of minor planet Names*. Springer.
- Scott, E. R., Keil, K., Goldstein, J. I., Asphaug, E., Bottke, W. F., & Moskovitz, N. A. (2015). Early impact history and dynamical origin of differentiated meteorites and asteroids. *Asteroids*, 4, 573–595.
- Shepard, M. K., Clark, B. E., Ockert-Bell, M., Nolan, M. C., Howell, E. S., Magri, C., et al. (2010). A radar survey of M-and X-class asteroids II. Summary and synthesis. *Icarus*, 208(1), 221–237. <https://doi.org/10.1016/j.icarus.2010.01.017>
- Shepard, M. K., de Kleer, K., Cambioni, S., Taylor, P. A., Virkki, A. K., Rivera-Valentin, E. G., et al. (2021). Asteroid 16 Psyche: Shape, features, and global map. *The Planetary Science Journal*, 2(4), 125. <https://doi.org/10.3847/psj/abfdab>
- Shepard, M. K., Richardson, J., Taylor, P. A., Rodriguez-Ford, L. A., Conrad, A., de Pater, I., et al. (2017). Radar observations and shape model of asteroid 16 Psyche. *Icarus*, 281, 388–403. <https://doi.org/10.1016/j.icarus.2016.08.011>
- Takir, D., Reddy, V., Sanchez, J. A., Shepard, M. K., & Emery, J. P. (2016). Detection of water and/or hydroxyl on asteroid (16) Psyche. *The Astronomical Journal*, 153(1), 31. <https://doi.org/10.3847/1538-3881/153/1/31>
- Tholen, D. J. (1984). *Asteroid taxonomy from cluster analysis of photometry* (Ph.D. thesis). University of Arizona.
- Unterborn, C. T., Desch, S. J., Haldemann, J., Lorenzo, A., Schulze, J. G., Hinkel, N. R., & Panero, W. R. (2023). The nominal ranges of rocky planet masses, radii, surface gravities, and bulk densities. *The Astrophysical Journal*, 944(1), 42. <https://doi.org/10.3847/1538-4357/aca3b>
- van Houten-Groeneveld, I., & van Houten, C. J. (1958). Photometric studies of asteroids. VII. *The Astrophysical Journal*, 127, 253. <https://doi.org/10.1086/146459>
- Weiss, B. P., & Elkins-Tanton, L. T. (2013). Differentiated planetesimals and the parent bodies of chondrites. *Annual Review of Earth and Planetary Sciences*, 41(1), 529–560. <https://doi.org/10.1146/annurev-earth-040610-133520>
- Weiss, B. P., Elkins-Tanton, L. T., Barucci, M. A., Sierks, H., Snodgrass, C., Vincent, J. B., et al. (2012). Possible evidence for partial differentiation of asteroid Lutetia from Rosetta. *Planetary and Space Science*, 66(1), 137–146. <https://doi.org/10.1016/j.pss.2011.09.012>
- Weiss, B. P., Merayo, J. M., Ream, J. B., Oran, R., Brauer, P., Cochrane, C. J., et al. (2023). The Psyche magnetometry investigation. *Space Science Reviews*, 219(3), 22. <https://doi.org/10.1007/s11214-023-00965-z>
- Zellner, B., & Gradie, J. (1976). Minor planets and related objects. XX. Polarimetric evidence for the albedos and compositions of 94 asteroids. *The Astronomical Journal*, 81, 262–280. <https://doi.org/10.1086/111882>
- Zolotov, M. Y. (2020). The composition and structure of Ceres' interior. *Icarus*, 335, 113404. <https://doi.org/10.1016/j.icarus.2019.113404>
- Zuber, M. T., Park, R. S., Elkins-Tanton, L. T., Bell, III, J. F., Bruvold, K. N., Bercovici, D., et al. (2022). The Psyche gravity investigation. *Space Science Reviews*, 218(8), 57. <https://doi.org/10.1007/s11214-022-00905-3>